DMD Fast Forward. Published on December 5, 2007 as doi:10.1124/dmd.107.019133

ENZYMATIC *C*-DEMETHYLATION OF 1-[2-(5-TERT-BUTYL-[1, 3, 4] OXADIAZOLE-2-CARBONYL)-4-FLUORO-PYRROLIDIN-1-YL]-2-(2-HYDROXY-1, 1-DIMETHYL-ETHYLAMINO)-ETHANONE IN RAT LIVER MICROSOMES

Hye Hyun Yoo, Hye Jin Chung, Jaeick Lee, Chang-Seok Lee, Min Jung Kang, and Dong-Hyun Kim

Doping Control Center, Korea Institute of Science and Technology, PO Box 131, Chungryang, Seoul 136-791, Korea: HHY, HJC, MJK, DHK

Bioanalysis and Mass Spectrometry, LG Life Sciences R&D, Taejon, Korea: JL, CSL

DMD Fast Forward. Published on December 5, 2007 as DOI: 10.1124/dmd.107.019133
This article has not been copyedited and formatted. The final version may differ from this version.

Running title: Enzymatic C-demethylation of LC15-0133 in rat liver microsomes

Correspondence: D-H Kim, Doping Control Center, Korea Institute of Science and Technology, PO Box 131, Chungryang, Seoul 136-791, Korea

Phone: + 82-2-958-5055; Fax: + 82-2-958-6677; E-mail: dhkim@kist.re.kr.

Number of text pages: 16

Number of Tables: 1

Number of Figures: 3

Number of Scheme: 1

Number of References: 13

Number of words in the *Abstract*: 117

Number of words in the *Introduction*: 173

Number of words in the *Discussion*: Results and Discussion: 1045

Abbreviations: DPP-4, dipeptidyl peptidase-4; GLP-1, glucagon-like peptide-1; GIP, gastric inhibitory polypeptide; ESI, electrospray ionization; CID, collision-induced dissociation; LC/MSD, liquid chromatography/mass selective detector.

DMD Fast Forward. Published on December 5, 2007 as DOI: 10.1124/dmd.107.019133
This article has not been copyedited and formatted. The final version may differ from this version.

Abstract

The *in vitro* metabolism of LC15-0133, a novel dipeptidyl peptidase-4 (DPP-4) inhibitor, was investigated using a hepatic microsomal system. The structures of the metabolites were characterized using mass spectral analysis and by comparison with synthetic references. The *in vitro* incubation of LC15-0133 with rat liver microsomes resulted in the formation of six metabolites, with the major metabolic reactions being hydroxylation and carbonyl reduction. Of the metabolites, a *C*-demethylated metabolite (M4) was identified, but was only detected in rat liver microsomes; experimental evidence revealed that the *C*-demethylated metabolite was generated by non-enzymatic decarboxylation of the carboxyl metabolite (M1). Non-enzymatic decarboxylation is postulated to occur due to the resonance stabilization by the oxadiazole ring attached to the *tert*-butyl moiety.

DMD Fast Forward. Published on December 5, 2007 as DOI: 10.1124/dmd.107.019133
This article has not been copyedited and formatted. The final version may differ from this version.

Introduction

LC15-0133 (1-[2-(5-tert-Butyl-[1, 3, 4] oxadiazole-2-carbonyl)-4-fluoro-pyrrolidin-1-yl]-2-(2-hydroxy-1, 1-dimethyl-ethylamino)-ethanone), a novel dipeptidyl peptidase-4 (DPP-4) inhibitor, is under development as a therapeutic agent for diabetes. DPP-4 inhibitors have been characterized to lower blood glucose in diabetic rodents via prolongation of glucagon-like peptide-1 (GLP-1) and the action of gastric inhibitory polypeptide (GIP) (Ahren and Schmitz, 2004; Demuth et al., 2005; Barnett, 2006; Campbell, 2007; Pratley and Salsali, 2007).

As a part of the pre-clinical study of LC15-0133, the *in vitro* metabolism of LC15-0133 was investigated using rat, dog and human liver microsomes. LC15-0133 was metabolized to 4-6 metabolites, via hydroxylation and carbonyl reduction, with considerable species difference noted in rat liver microsomes. *C*-demethylated and carboxy metabolites were observed only in the rat liver microsomal incubation. Because the *C*-demethylation reaction is not a common enzymatic reaction, the metabolic pathway for the generation of the *C*-demethylated metabolite requires further investigation.

The purpose of the present study was to characterize the *in vitro* metabolism of LC15-0133 and identify the mechanism of the rat liver microsomal enzyme catalyzed

C-demethylation reaction of LC15-0133.

Materials and methods

Chemicals. LC15-0133 and LC15-0133-d_6 (IS), with a chemical purity > 99%, were provided by LG Life Sciences R&D (Daejon, Korea). Authentic standards of LC15-0133 metabolites (M3, M4, and M5), with chemical purity >95%, were also provided by LG Life Sciences R&D (Daejon, Korea). All other chemicals were the highest grade commercially available.

Microsomes. Human liver microsomes were purchased from BD Biosciences (MA, USA). Rat liver samples were taken from Sprague-Dawley rats (Daehan Animal, Daejeon, Korea) and dog liver samples from Beagle dogs (Daehan Animal, Daejeon, Korea). The microsomal fraction was prepared according to the method previously described elsewhere (Guengerich et al., 1986).

In vitro microsomal incubation. LC15-0133 (100 μM final concentration) was incubated with 2 mg/mL liver microsomes, at 37 ºC for 2 hr, in the presence of an NADPH generating system (10 mM glucose 6-phosphate, 0.67 mM β-$NADP^+$ and 1 U/ml glucose 6-phosphate dehydrogenase), in a final incubation volume of 200 μL. The reaction was terminated by the addition of 400 μL of 0.1% acetic acid, with 50 μL of

LC15-0133-d_6 (10 μg/mL) added as an internal standard solution. The samples were then passed through activated Sep-Pak C_{18} cartridges (96-well type OASIS HLB extraction cartridge), washed twice with 1 mL of distilled water, and eluted with 1 mL of methanol. The methanol eluate was dried under nitrogen gas. The residue was redissolved in 50 μL acetonitrile, with 10 μL injected on to an HPLC column for HPLC/MS analyses.

LC/MS analysis. The HPLC/MS system consisted of an HP 1100 series binary pump HPLC system (Agilent, Palo Alto, CA, USA), with a diode array detector (Agilent) and LC/MSD ion-trap mass spectrometer, equipped with an electrospray ionization source (Agilent). The chromatographic separation of LC15-0133 and its metabolites was achieved on a Capcell-Pak C_8 column (2.0 mm × 15 cm, 5 μm, Shiseido), using a linear gradient program. The mobile phases consisted of 10 mM ammonium formate at pH 6.0 (A) and 90% acetonitrile (B). The initial composition was 15% (B), programmed linearly to 65% (B) over 15 min, at a flow rate of 0.2 mL/min. Mass spectrometry and tandem mass spectrometry analyses were performed using a LC/MSD ion trap mass spectrometer. The entire column eluent was directly introduced into an electrospray ionization (ESI) interface, via a 50-cm long section of PEEK tubing (0.13 mm i.d.). Nitrogen was used as both the nebulizing and drying gas at 35 psi and a

flow rate of 8 L/min, respectively, with a temperature of 350 ºC. The mass spectrometer was operated in the positive ion mode. Helium was used as the collision gas for the tandem mass spectrometric experiments. Fragmentation was induced with a resonant excitation amplitude of 0.85, following isolation of the desired precursor ion over a selected mass window of 1 Da. All instrumental controls and data processing were performed using the LC/MSD Trap Software (ver. 4.1).

Results and discussion

A representative extracted ion chromatogram obtained from the analysis of rat liver microsomal incubation is shown in Fig. 1. The incubation of LC15-0133 with rat liver microsomes in the presence of the NADPH-generating system yielded six different metabolites, the protonated molecular ions of which were observed at *m/z* 401, 403, 387, 357 and 373.

The structures of LC15-0133 and its metabolites were characterized, and assigned based on their product ion mass spectra and fragmentation patterns obtained from collision-induced dissociation (CID) ion trap mass spectrometry. Metabolites M3, M4 and M5 were further confirmed by comparison with authentic compounds. The protonated molecular and characteristic product ions of LC15-0133 and its metabolites,

along with HPLC retention times, are summarized in Table 1. The $[M+H]^+$ ion of LC15-0133 was observed at m/z 371, with the MS^2 spectrum of this ion giving rise to major product ions at m/z 353, 299, 242 and 127. The product ions at m/z 299 and 242 were rationalized as sequential loss of a tert-hydroxybutyl group and aminomethylcarbonyl moiety, with that at m/z 127 as cleavage of the tert-butyloxazole moiety (Fig. 2A).

Metabolite M3 produced a protonated molecule at *m/z* 387, indicating this compound was a mono-hydroxylated derivative of LC15-0133. M3 generated characteristic product ions at *m/z* 369, 315, 258 and 143, these being 16 Da higher than those of the corresponding product ions at *m/z* 353, 299, 242 and 127 of LC15-0133 (Table 1). These characteristic product ions indicated hydroxylation of the *tert*-butyl moiety attached to oxadiazole ring.

The $[M+H]^+$ ion of M1 was observed at m/z 401, which gained 30 Da from that of protonated LC15-0133, and the MS^2 spectrum yielded product ions at m/z 357, 247 and 228. This metabolite was postulated to be a carboxylic acid derivative generated due to further oxidation of M3. The product ion at m/z 357 was postulated to have been generated due to dissociation of a carboxyl moiety from the protonated molecular ion. The MS^3 spectrum of the ion at m/z 357 was consistent with the MS^2 spectrum of M4,

DMD Fast Forward. Published on December 5, 2007 as DOI: 10.1124/dmd.107.019133
This article has not been copyedited and formatted. The final version may differ from this version.

the *C*-decarboxylated metabolite (Fig 2B and 2C), which strongly indicated that M1 was a carboxylic acid metabolite.

M5 and M6 produced $[M+H]^+$ ions at m/z 373, and both generated characteristic product ions at m/z 355, 301, 283, 244 and 175, suggesting that M6 was a stereoisomer of M5. The protonated molecular and the product ions of these metabolites were 2 Da higher than those of the corresponding ions of the parent compounds, suggesting these metabolites were carbonyl reduced metabolites. M2 produced a $[M+H]^+$ ion at *m/z* 403, which was 32 Da higher relative to that of LC15-0133, with major product ions at *m/z* 385 and 357. This metabolite was postulated to be a dihydroxylated metabolite. M4 generated a $[M+H]^+$ ion at *m/z* 357, which was 14 Da less than that of LC15-0133, suggesting that this metabolite was a demethylated derivative. All the product ions were also 14 Da less than the corresponding ions of the parent compounds, suggesting demethylation had occurred at the tert-butyl moiety. The structure of M4 was confirmed by comparison with a synthetic standard.

The structure of M4 was somewhat unexpected, as *C*-demethylation is not common during metabolism; whereas, *O*- and *N*-demethylations are frequently observed in the biotransformation of xenobiotics (Coutts et al., 1994; Burke et al., 1994; Ertl et al., 1999). In case of terfenadine possessing a *tert*-butyl moiety on the backbone of the

compound, similarly to LC15-0133, both alcohol and acid metabolites have been identified, but the *C*-demethylated metabolite has never been reported (Jurima-Romet et al., 1994; Terhechte and Blaschke, 1995; Ling et al., 1995; Rodrigues et al., 1995). Initially, it was postulated that M4 was able to be generated via the sulfate conjugate of M1, from which the carboxyl sulfate moiety might easily be dissociated. However, this possibility was ruled out as not even trace amount of a sulfate conjugate was detected in the incubation along with phosphoadenosyl phosphosulfate (data not shown).

It was subsequently hypothesized that the *C*-demethylated metabolite (M4) could be spontaneously generated from the acid metabolite (M1) via decarboxylation, where the removal of the carboxyl group was attributed to the oxadiazole ring attached to the *tert*-butyl moiety. To test this hypothesis, the acid metabolite (M1) was collected using preparative HPLC, treated and then re-injected under different conditions. The treatment of M1 under high pH or high temperature conditions accelerated the formation of M4, supporting that the *C*-demethylated metabolite was generated by the non-enzymatic decarboxylation of M1 (Fig. 3).

The oxadiazole ring attached to the *tert*-butyl moiety supposedly contributes to the resonance, which stabilizes the electrons by conjugation, for decarboxylation of the *tert*-butyl site. As shown Scheme 1, the electron pairs forming the oxygen-hydrogen bond in

the carboxyl group of M1 might be stabilized over the oxadiazole ring up to the carbonyl group. This resonance stabilization would facilitate the decarboxylation in M1. For testing this hypothesis, we carried out microsomal incubation of M3 in D_2O-medium. On the assumption that M4 is formed from M3 via an intermediate of an arylketone enolate, the metabolite of which isopropyl proton was replaced with deuterium was expected to be detected as deuterium would be inserted to the tertiary carbon of isopropyl group in the intermediate form of arylketone enolate. When M3 was incubated in D_2O-medium, the MS spectrum corresponding to peak of M4 showed major ion at *m/z* 358 instead of *m/z* 357 as expected (Supplement 1). This data proved indirectly that M4 was formed from an intermediate of an arylketone enolate as postulated.

A considerable amount of the *C*-demethylated metabolite, M4, (~10% of the parent drug found) was observed in the urine and plasma samples from rats administered LC15-0133 (data not shown). The apparent kinetic parameters for M4 formation from LC15-0133 in rat liver microsomes were K_m of 72.9 μM and V_{max} of 5.03 pmol/min/mg protein (Supplement 2). However, neither the acid or demethylated metabolite (M1 & M4, respectively) was found in the incubations with dog and human liver microsomes (Supplement 3), which suggests this biotransformation reaction; alcohol to carboxylic

DMD Fast Forward. Published on December 5, 2007 as DOI: 10.1124/dmd.107.019133
This article has not been copyedited and formatted. The final version may differ from this version.

acid, is species-specific. The research on the enzyme(s) involved in carboxyl formation is on progress to identify which enzyme reaction is species-specific.

In conclusion, LC15-0133 was metabolized to a carboxylic acid metabolite, via an alcohol metabolite, by rat microsomal enzyme, which subsequently decarboxylated to yield a demethylated metabolite at the *tert*-butyl moiety. This unusual C-demethylation reaction was thought to occur due to the resonance stabilization due to the oxadiazole ring attached to the *tert*-butyl moiety.

Acknowledgements

The authors would like to thank Dr. D. Y. Shin (KIST, Seoul, Korea) for his helpful suggestion.

References

Ahren B and Schmitz O (2004) GLP-1 receptor agonists and DPP-4 inhibitors in the treatment of type 2 diabetes. *Horm Metab Res* 36: 867–876.

Barnett A (2006) DPP-4 inhibitors and their potential role in the management of type 2 diabetes. *Int J Clin Pract* 60: 1454–1470.

Burke MD, Thompson S, Weaver RJ, Wolf CR and Mayer RT (1994) Cytochrome P450 specificities of alkoxyresorufin O-dealkylation in human and rat liver. *Biochem Pharmacol* 48: 923–936.

Campbell RK (2007) Rationale for dipeptidyl peptidase 4 inhibitors: a new class of oral agents for the treatment of type 2 diabetes mellitus. *Ann Pharmacother* 41: 51–60.

Coutts RT, Su P and Baker GB (1994) Involvement of CYP2D6, CYP3A4, and other cytochrome P-450 isozymes in N-dealkylation reactions. *J Pharmacol Toxicol Methods* 31: 177–186.

Demuth HU, McIntosh CH and Pederson RA (2005) Type 2 diabetes–therapy with dipeptidyl peptidase IV inhibitors. *Biochim Biophys Acta* 1751: 33–44.

Ertl RP, Alworth WL and Winston GW (1999) Liver microsomal cytochromes P450-dependent alkoxyphenoxazone O-dealkylation in vitro by alligator and rat: activities, inhibition, substrate preference, and discrimination factors. *J Biochem Mol Toxicol*

13: 17–27.

Guengerich FP, Martin MV, Beaune PH, Kremers P, Wolff T and Waxman DJ (1986) Characterization of rat and human liver microsomal cytochrome P-450 forms involved in nifedipine oxidation, a prototype for genetic polymorphism in oxidative drug metabolism. *J Biol Chem* 261: 5051–5060.

Jurima-Romet M, Crawford K, Cyr T and Inaba T (1994) Terfenadine metabolism in human liver. In vitro inhibition by macrolide antibiotics and azole antifungals. *Drug Metab Dispos* 22: 849–857.

Ling KH, Leeson GA, Burmaster SD, Hook RH, Reith MK and Cheng LK (1995) Metabolism of terfenadine associated with CYP3A(4) activity in human hepatic microsomes. *Drug Metab Dispos* 23: 631–636.

Pratley RE and Salsali A (2007) Inhibition of DPP-4: a new therapeutic approach for the treatment of type 2 diabetes. *Curr Med Res Opin* 23: 919–931.

Rodrigues AD, Mulford DJ, Lee RD, Surber BW, Kukulka MJ, Ferrero JL, Thomas SB, Shet MS and Estabrook RW (1995) In vitro metabolism of terfenadine by a purified recombinant fusion protein containing cytochrome P4503A4 and NADPH-P450 reductase. Comparison to human liver microsomes and precision-cut liver tissue slices. *Drug Metab Dispos* 23: 765–775.

Terhechte A and Blaschke G (1995) Investigation of the stereoselective metabolism of the chiral H1-antihistaminic drug terfenadine by high-performance liquid chromatography. *J Chromatogr A* 694: 219–225.

Footnotes

This work was supported in part by grant from LG Life Sciences R&D and in part by intramural grant from Korea Institute of Science and Technology.

DMD Fast Forward. Published on December 5, 2007 as DOI: 10.1124/dmd.107.019133
This article has not been copyedited and formatted. The final version may differ from this version.

Legends for figures

Fig. 1. Extracted ion chromatograms for LC15-0133 and its metabolites in the incubation mixture with rat liver microsomes.

Fig. 2. MS^2 spectra and the postulated fragmentation patterns for (A) LC15-0133, (B) M1 and (C) M4. The embedded spectrum in B is the MS^3 spectrum for *m/z* 401→357 ions.

Fig. 3. Extracted ion chromatograms of the M1-containing fraction after incubation at pH 4 (A), pH 7.4 (B) and pH 9 (C), and at 50˚C (D). The fraction containing M1 was collected after separation of the microsomal incubation mixture by HPLC, which was further incubated for 30 min under the conditions described above, and then re-injected onto the column.

DMD Fast Forward. Published on December 5, 2007 as DOI: 10.1124/dmd.107.019133
This article has not been copyedited and formatted. The final version may differ from this version.

Table 1

Protonated molecular and characteristic product ions for LC15-0133 and its associated metabolites

Compound	RT	$[M+H]^+$	MS/MS fragmentation
LC15-0133	12.0	371	353, 299, 281, 242, 173, 127
M1	3.5	401	357, 247, 228
M2	6.1	403	385, 357, 313, 285, 263, 228
M3	8.5	387	369, 340, 315, 258, 173. 143
M4	10.3	357	339, 285, 267, 228, 173, 113
M5	10.7	373	355, 301, 283, 244, 214, 175, 157
M6	10.7	373	355, 301, 283, 244, 214, 175, 157

DMD Fast Forward. Published on December 5, 2007 as DOI: 10.1124/dmd.107.019133
This article has not been copyedited and formatted. The final version may differ from this version.

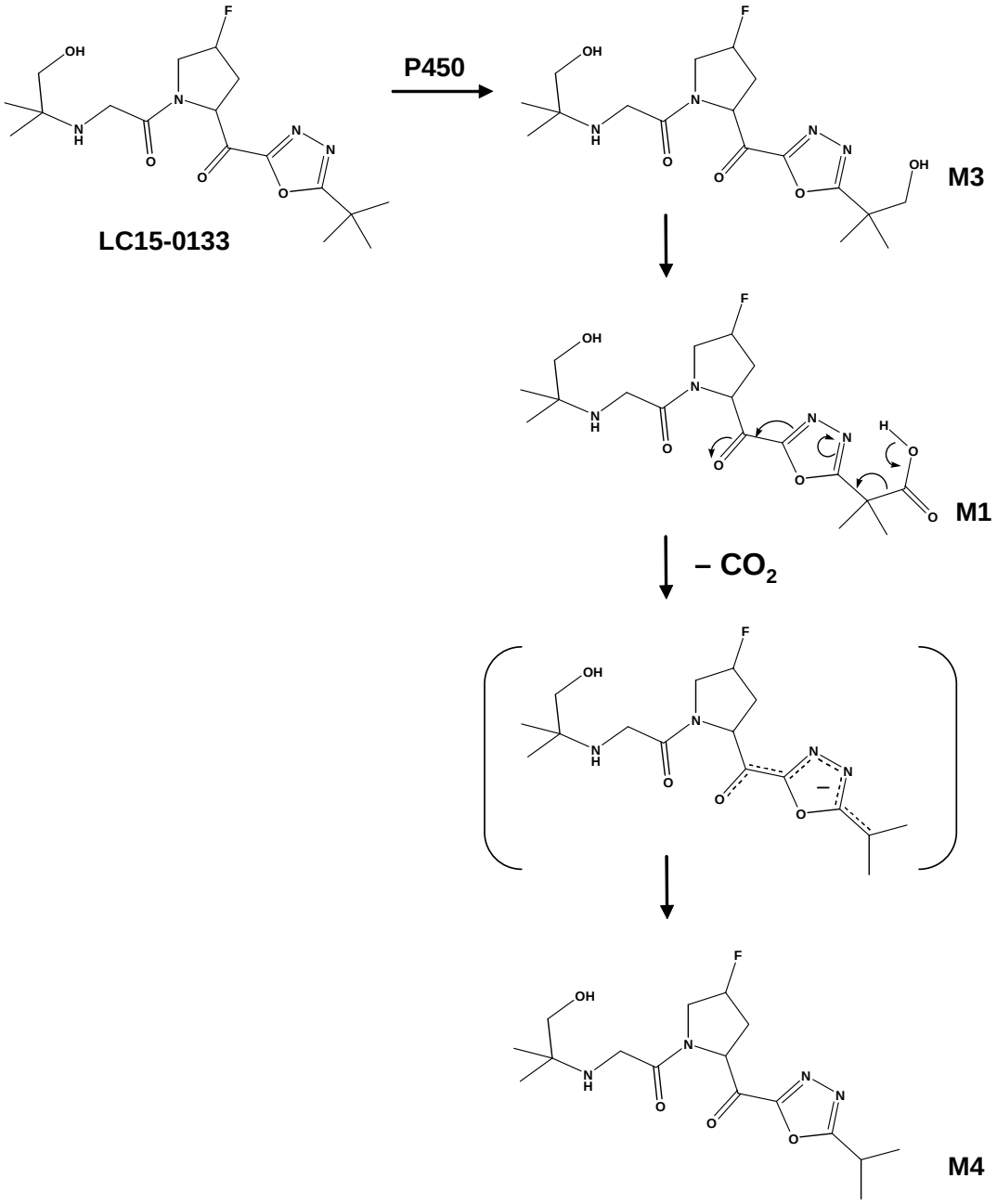

Scheme 1. Proposed metabolic pathway of LC15-0133 toward M4

DMD Fast Forward. Published on December 5, 2007 as DOI: 10.1124/dmd.107.019133
This article has not been copyedited and formatted. The final version may differ from this version.

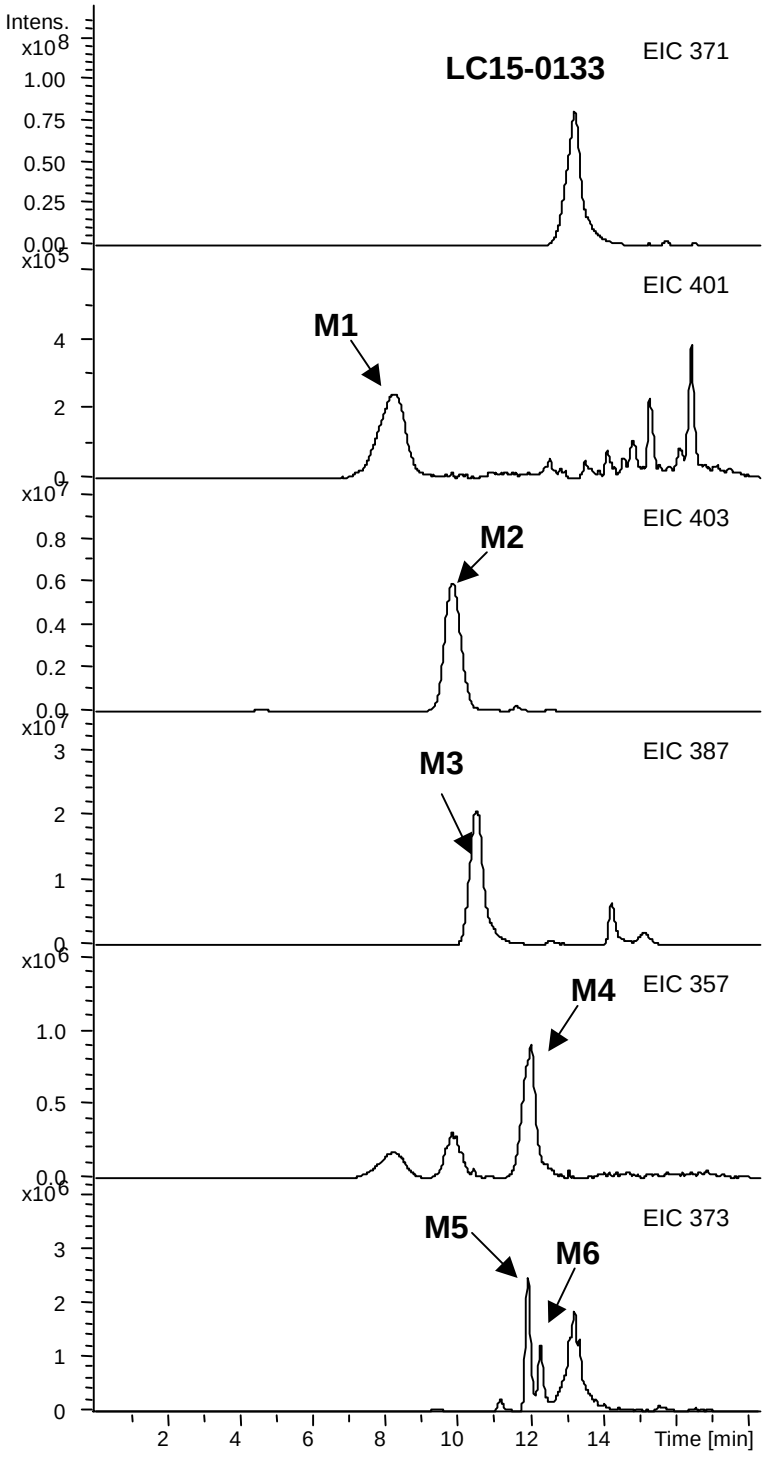

Fig. 1

DMD Fast Forward. Published on December 5, 2007 as DOI: 10.1124/dmd.107.019133
This article has not been copyedited and formatted. The final version may differ from this version.

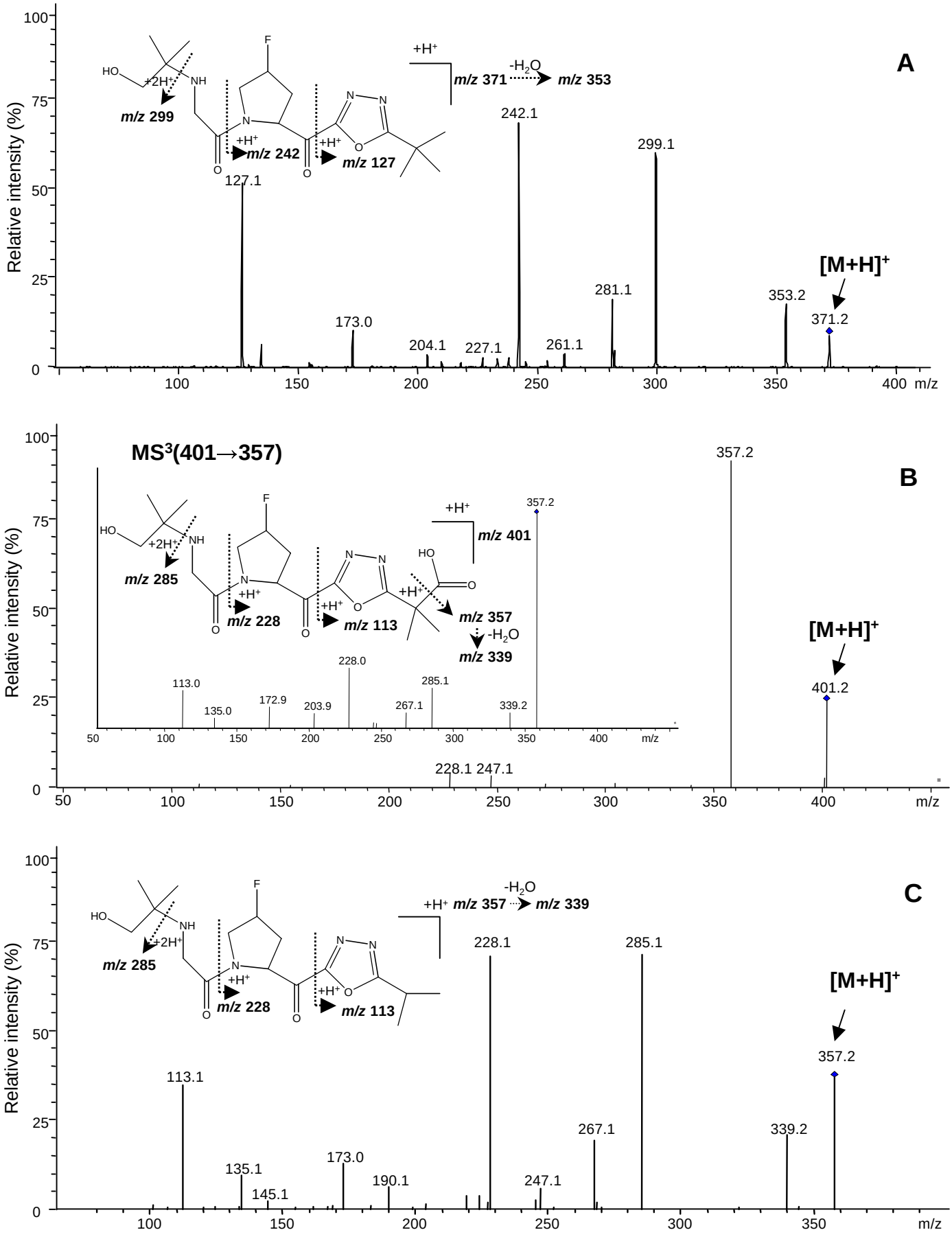

Fig. 2

DMD Fast Forward. Published on December 5, 2007 as DOI: 10.1124/dmd.107.019133
This article has not been copyedited and formatted. The final version may differ from this version.

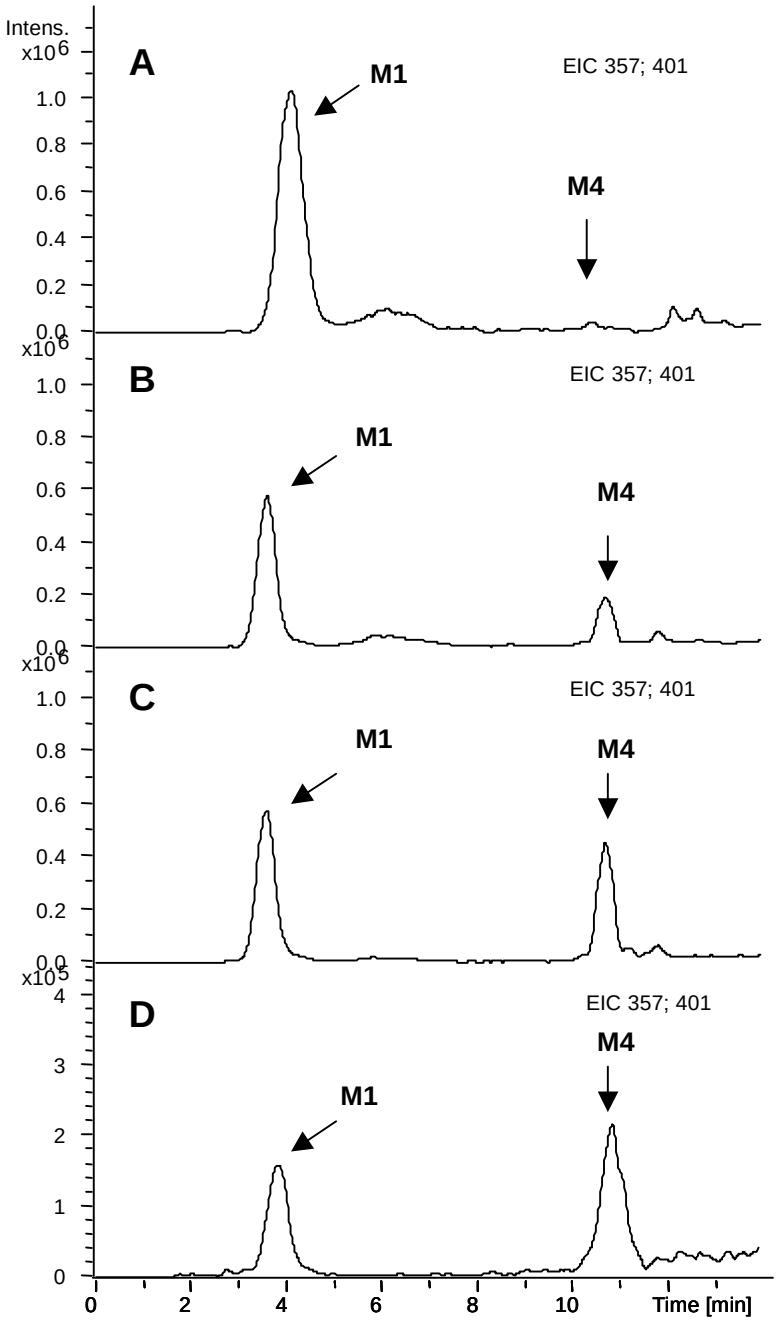

Fig. 3